Mazumdar, S., Long, Z., and Chen, Q. 2014. "A coupled CFD and analytical model to simulate airborne contaminant transmission in cabins" *Indoor and Built Environment*, 23, 946-954.

A coupled CFD and analytical model to simulate airborne contaminant transmission in cabins

Sagnik Mazumdar[a], Zhenwei Long[b*], Qingyan Chen[a,b]

[a] School of Mechanical Engineering, Purdue University, West Lafayette, IN 47907, USA
[b] School of Environmental Science and Engineering, Tianjin University, Tianjin 300072, China

[*]Phone: +86-22-2740 9500, Email: longzw@tju.edu.cn

Abstract

A coupled CFD and analytical model is presented for accurate and time-efficient prediction of transient airborne contaminant transmission in full-length airliner cabins. The CFD model was used at locations near the contaminant source, while the analytical model was used for the rest of the cabin. The coupling at the interface of the CFD and the analytical model to solve the transient contaminant flux used two different methods. One method forced an outflow condition at the interface of the CFD; this analytical model is less accurate but easier to implement in commercial CFD software. The other method that iteratively solved the contaminant flux at the interface is more accurate but is computationally intensive. A procedure to analytically calculate the contaminant concentration using the transient contaminant flux condition at the interface is also developed.

Keywords: Analytical model, CFD, Coupling, Contaminant transport, Cabins

Introduction

Within months after its emergence in rural China, SARS affected more than 8000 patients and caused 774 deaths in 26 countries on five continents [1]. The potential of air travel to globally disseminate an emerging infectious disease makes it an important public health issue [2]. Airborne infectious diseases transmitted in airliners in recent years include SARS, tuberculosis, influenza, measles, and mumps [3,4]. Investigations on in-flight transmission of airborne disease contaminants have been done using experimental measurements and computer simulations. Experimental measurements provide the most realistic information, but such studies are very expensive, time consuming, and difficult [5-7]. On the other hand, computer simulations using Computational Fluid Dynamics (CFD) simulation take a few weeks of computing time to study only a few minutes of transient contaminant transport in a full length airliner cabin even with a computer cluster [8]. In some cases, a simplified model is preferred because it produces good estimate of the air and contaminant distributions with minimal costs [9].

For example, Zhai and Metzger [10] developed methods that can rapidly identify optimal system parameters based on the Taguchi method and CFD. Other simplified and fast approaches include use of Zonal models [11], Coarse-grid CFD [12], Fast Fluid Dynamics (FFD) [13] and Artificial Neural Network models [14]. Graphics Processing Unit (GPU) is also envisioned as an option for faster computation as it can be 500-1500 times faster than the CFD on a CPU [13]. Mazumdar and Chen [15] developed a fast and effective one-dimensional analytical model to study airborne contaminant transmission inside full-length airliner cabins. The model assumed complete mixing of contaminants in the cabin cross section due to the high air exchange rates [16]. Experimental measurements [17] and CFD simulations [15] show that this assumption is not appropriate at locations near the contaminant source, as local airflow plays a predominant role in how the contaminant is distributed. So to capture the effects of the local flow in contaminant distribution, coupling CFD with a one-dimensional analytical model was proposed [15]. CFD would be used at locations near the contaminant source, while the analytical model would be used for the rest of the cabin where the uniform mixing assumption is more valid. The coupled technique is a computationally time-efficient method for contaminant transport simulations in a full length airliner cabin without much loss of accuracy.

A coupled method was used by Mazumdar and Chen [15] to predict steady state contaminant distribution for a continuously releasing contaminant source such as breathing. However, most contaminant release processes such as coughing and sneezing are transient. This paper developed the coupled CFD and analytical model further to address more general transient contaminant transmission scenarios in airliner cabins.

Model Development

To further develop the coupled CFD and analytical model, this investigation used a fully-occupied airliner cabin, as shown in Fig. 1. The method used a transient contaminant source at row N and assumed that the CFD model was applied for rows N-1, N and N+1. This study further assumed that the airflow in the cabin was steady for the analytical domain. A steady airflow field can be obtained using CFD with periodic boundary conditions at interfaces 1 and 2. With the computed flow field, the local contaminant transmission in the CFD domain can be solved if the contaminant flux, $S_{\varphi 2}$ (kg/s), at the interface of the CFD and the analytical model is known.

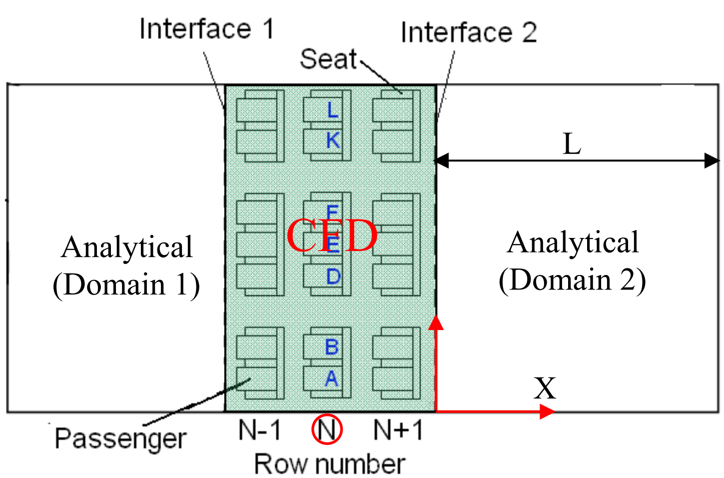

Fig. 1. Schematic of the coupled model

For the analytical domain, the governing contaminant transmission equation is:

$$\frac{\partial C}{\partial t} = D\frac{\partial^2 C}{\partial x^2} - V_L\frac{\partial C}{\partial x} - \lambda\left(C - C_{inlet}\right) \tag{1}$$

where D is a modified diffusion coefficient, V_L is the longitudinal velocity of airflow inside of the cabin, C_{inlet} is the contaminant concentration coming in through the inlet, and λ is a factor of several cabin features such as flow rate inside the cabin and area of cross-section of the cabin (A_c) [15]. Both the D and V_L can be obtained from a single row cabin CFD simulation [15].

The boundary condition at interface x=0 is:

$$-\Gamma A_c\frac{\partial C}{\partial x} + \rho A_c V_L C = S_{\varphi 2} \tag{2}$$

while the initial condition at t= 0 is:

$$C(x,0) = F(x) \tag{3}$$

assuming that an initial amount of contaminant already exists inside the cabin. This initial concentration assumption is effectively used to balance the transient contaminant flux condition, which would become evident later, at the interface.

By using the principle of superposition [18-20], *C(x,t)* can be redefined as:

$$C\left(x,t\right) = C_1\left(x\right) + C_2\left(x,t\right) \tag{4}$$

where:

$$C_1(x) = Ae^{m_1 x} + Be^{m_2 x} + C_{inlet} \tag{5}$$

with:

$$m_1 = \frac{V_L + \sqrt{V_L^2 + 4\lambda D}}{2D}\ ;\ m_2 = \frac{V_L - \sqrt{V_L^2 + 4\lambda D}}{2D}$$

$$A = -\frac{\omega_2\omega_4}{\omega_1 - \omega_4}S_{\varphi 2} + \frac{\omega_1\omega_5 - \omega_4\omega_3}{\omega_1 - \omega_4}C_{inlet}$$

$$B = \frac{\omega_2}{\omega_1 - \omega_4}S_{\varphi 2} + \frac{\omega_3 - \omega_5}{\omega_1 - \omega_4}C_{inlet}$$

$$\omega_1 = \frac{\left[-\Gamma m_2 + \rho V_L\right]}{\left[-\Gamma m_1 + \rho V_L\right]}\ ;\ \omega_2 = \frac{1}{\left[-\Gamma A_c m_1 + \rho A_c V_L\right]}\ ;\ \omega_3 = -\frac{\rho V_L}{\left[-\Gamma m_1 + \rho V_L\right]}$$

$$\omega_4 = \frac{\left[\Gamma m_2 + \rho V_L\right]}{\left[\Gamma m_1 + \rho V_L\right]} e^{(m_2 - m_1)L} \quad ; \quad \omega_5 = -\frac{\rho V_L}{\left[\Gamma m_1 + \rho V_L\right] e^{m_1 L}}$$

C_2 can be solved using the method of separation of variables [18-20]:

$$\begin{aligned} C_2(x,t) &= X(x)T(t) \\ &= a_0 e^{-\beta_0^2 t} + 2 \sum_{n=1}^{\infty} a_n \cos(\alpha_n x)\, e^{-\beta_n^2 t} \quad \text{if } V_L = 0 \\ &= 2\, e^{\frac{V_L}{2D}} \sum_{n=1}^{\infty} a_n \cos(\alpha_n x)\, e^{-\beta_n^2 t} \quad \text{if } V_L \neq 0 \end{aligned} \tag{6}$$

where:

If $V_L = 0$:

$$\alpha_n = \frac{n\pi}{L} \; ; \; \beta_n^2 = \lambda + \alpha_n^2 D \; ; \; a_0 = \frac{1}{L}\int_0^L \left[F(x) - C_1(x)\right] dx \; ; \; a_n = \frac{1}{L}\int_0^L \left[F(x) - C_1(x)\right] \cos\frac{n\pi x}{L}\, dx$$

If $V_L \neq 0$:

$$\alpha_n \cot(\alpha_n L) - \frac{D}{2V_L}\alpha_n^2 + \frac{V_L}{2D} = 0 \; ; \; \beta_n^2 = \lambda + \alpha_n^2 D + \frac{V_L^2}{4D} \quad (\alpha_n > 0)$$

$$\left[a_n\right]_{1 \le n \le \infty} = \left[R_m\right]_{1 \le m \le \infty} \left[L_{m,n}\right]_{1 \le m,n \le \infty}^{-1}$$

$$R_m = \int_0^L \left[F(x) - C_1(x)\right] \cos(\alpha_m x)\, dx$$

$$L_{m,n} = 2 e^{\frac{V_L}{2D}} \int_0^L \cos(\alpha_m x) \cos(\alpha_n x)\, dx$$

Assuming that a constant contaminant flux of $S_{\varphi 2}$ (kg/s) enters the analytical domain 2 from the CFD domain through interface 2, the contaminant concentration in the analytical domain can be calculated from:

$$\begin{aligned} C &= C_{inlet} + A e^{m_1 x} + B e^{m_2 x} + a_0 e^{-\beta_0^2 t} + 2 \sum_{n=1}^{\infty} a_n \cos(\alpha_n x)\, e^{-\beta_n^2 t} \quad \text{if } V_L = 0 \\ &= C_{inlet} + A e^{m_1 x} + B e^{m_2 x} + 2\, e^{\frac{V_L}{2D}} \sum_{n=1}^{\infty} a_n \cos(\alpha_n x)\, e^{-\beta_n^2 t} \quad \text{if } V_L \neq 0 \end{aligned} \tag{7}$$

The next paragraph will present methods for obtaining the contaminant flux of $S_{\varphi 2}$ (kg/s) at the interface. The contaminant concentration in Domain 1 can also be solved in a similar way. Moreover, C_{inlet} will depend on the net outflow of the contaminant from the analytical and the CFD domain.

Hereafter, depending on how it is handled in CFD, the contaminant flux, $S_{\varphi 2}$, at the interface can be obtained by two methods:

1. Interfaces 1 and 2 can be treated as outflow boundaries for the contaminant ($\partial C/\partial x = 0$) for the CFD simulations. This treatment could introduce an error to the analytical solution, but it is simple to implement.

2. The net flux (diffusive and convective) of a contaminant leaving from Interfaces 1 and 2 of the CFD model ($\int (-\Gamma \partial C/\partial x + \rho VC)\, dA = S_{\varphi 2}$) is equal to that entering the analytical domain ($S_{\varphi 2} = -\Gamma A_c\, \partial C/\partial x + \rho V_L A_c C$). This physical coupling method is accurate, but it is complicated to couple it with CFD software at the interfaces. For example, when commercial CFD program ANSYS Fluent [20] is used, an iterative user-defined function needs to be implemented to balance the net flux. Also note, Method 1 is a simplified case of Method 2 with zero gradients at the interfaces.

Model Implementation

This section outlines the implementation algorithm for the two coupling methods along with the procedure to solve the contaminant flux, $S_{\varphi 2}$, at the interface.

Fig. 2 shows the algorithm for Method 1. At each time step, the CFD model is first used to solve the contaminant distribution in the CFD zone with outflow condition at the interfaces. Once a converged CFD solution is obtained, the contaminant concentration flux, $S_{\varphi 2}$, can directly be calculated at the interface. The flux is then used as the boundary condition for the analytical model to obtain the contaminant distribution in the analytical domains. Note that in Fig. 2, the contaminant concentration, $C(x,t)$, depends on the CFD time step (Δt) and not on time (t). The concentration at time t is computed using the contaminant concentration at the previous time step ($F(x)= C(x,t-\Delta t)$). This is done to take care of the transient contaminant flux at the interface. The method assumes that the contaminant flux at the interface is a constant from time $t-\Delta t$ to t so that an analytical solution can be obtained. The algorithm saves the derived concentration equation at time t ($F(x)$) to compute the contaminant distribution in the next time step $t+\Delta t$. Since Method 1 does not have physical coupling between the two domains, it is easy to implement in any commercial CFD software.

Fig. 3 shows the implementation algorithm for Method 2. The analytical and CFD model is physically coupled as the contaminant flux, $S_{\varphi 2}$, is obtained iteratively to match the concentration at the interface. A good guess for the initial value of $S_{\varphi 2}$ is required for fast convergence. At t = 0 s, $S_{\varphi 2}$ can be set to zero, while at t = t, the initial value of $S_{\varphi 2}$ can be the value at $t = t-\Delta t$. The initial $S_{\varphi 2}$ is then used to compute the contaminant distribution in the CFD domain by the CFD model and in the analytical domain by the analytical model. The normalized difference in contaminant concentrations computed at the interface (ε) by the two models is then compared. The lower the value of ε, the more accurate is the coupled model. If ε is smaller than a predefined user criterion, then the solution is moved to the next time step. Otherwise, the flux $S_{\varphi 2}$ is modified and the whole process is repeated. The Newton-Raphson scheme is used to speed up the convergence of the contaminant flux at the interface of the two domains for this study [22]. However other schemes are also available which might result in faster convergence; they are left to be the scope for future studies. Moreover, note that ε should be judiciously selected by the user, as a very low value can make this physically coupled model as computationally time-consuming as CFD.

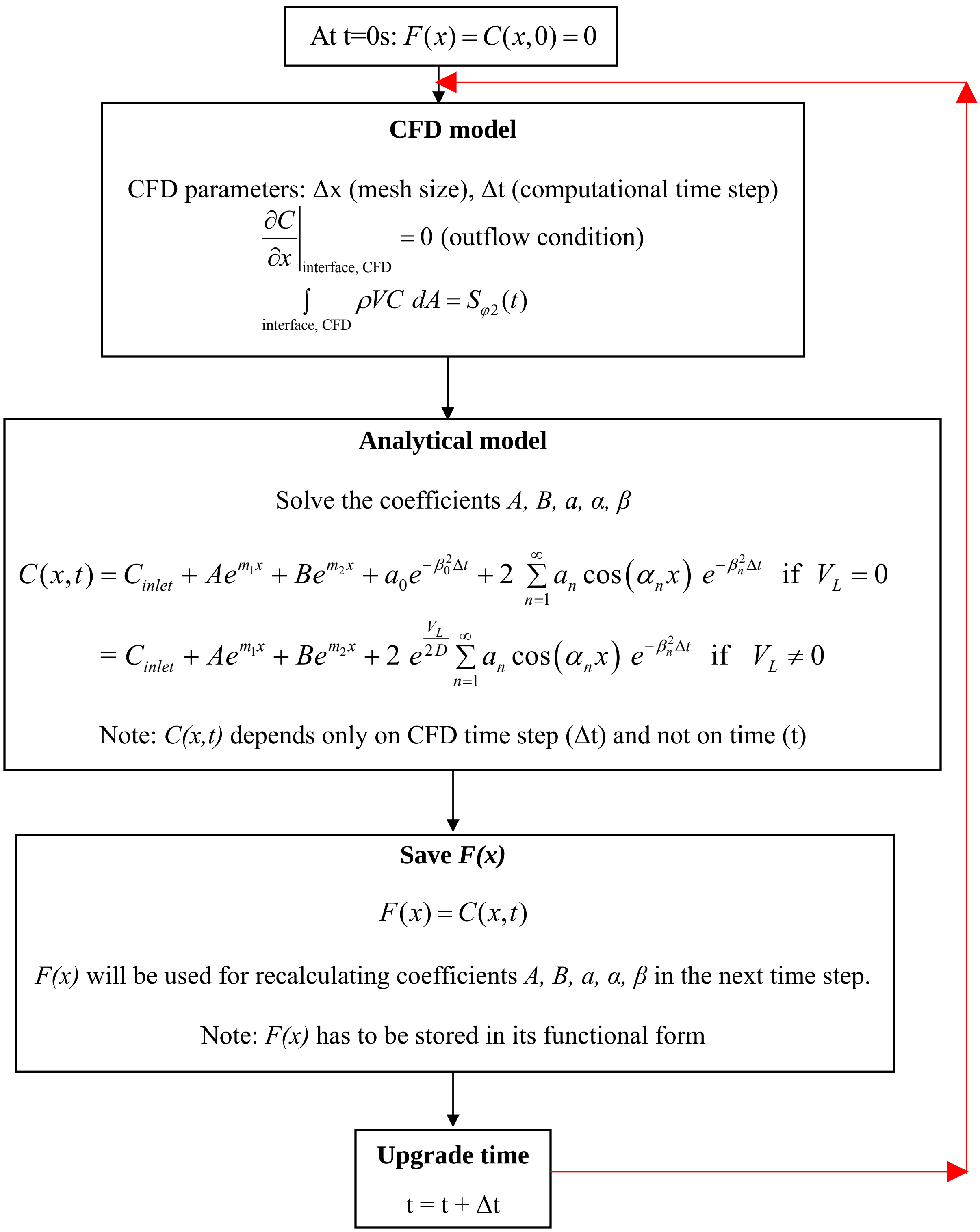

Fig. 2. Algorithm to implement coupling Method 1

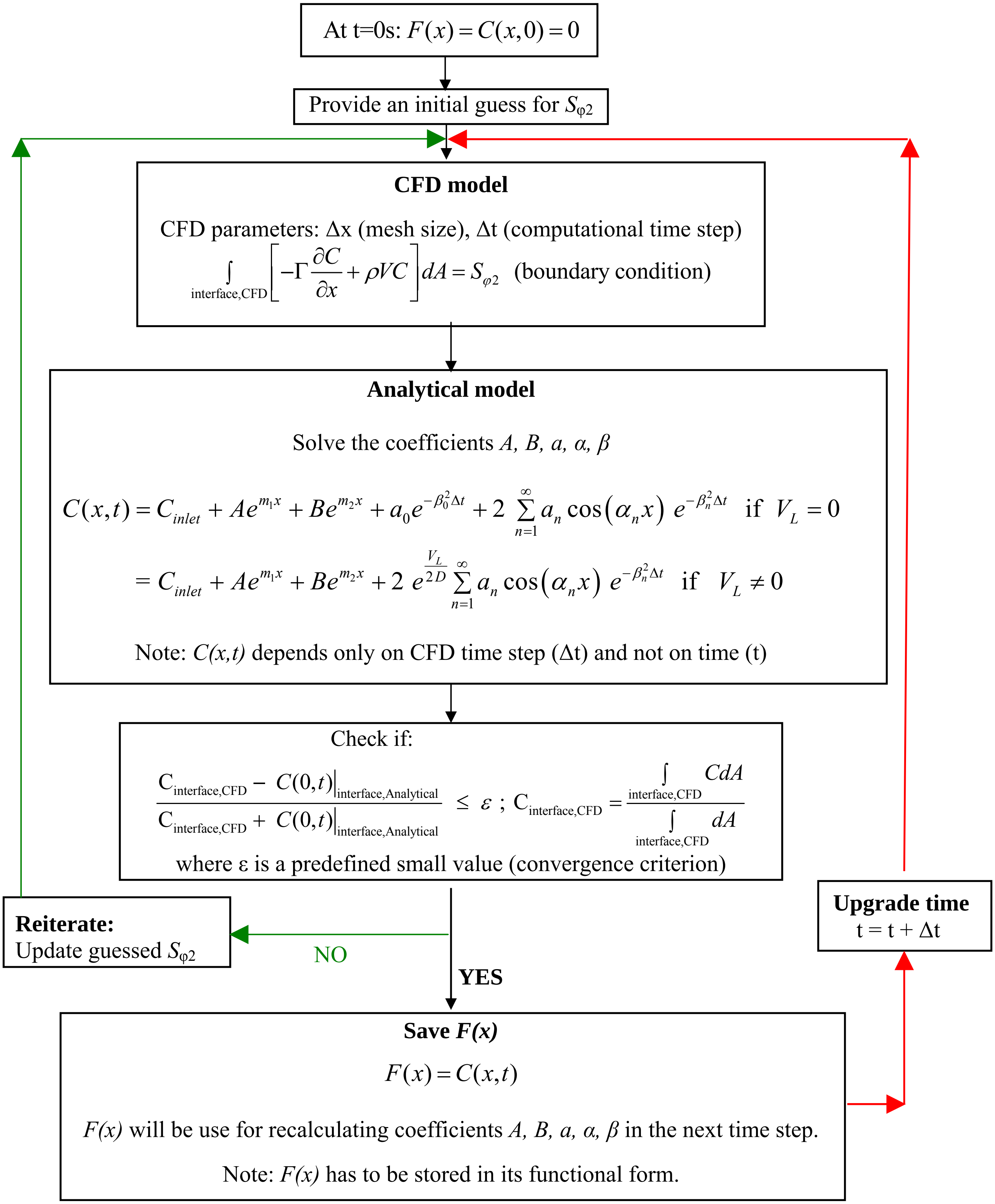

Fig. 3. Algorithm to implement coupling Method 2

Method 2 should be more accurate than Method 1, as no artificial boundary condition is imposed at the interface. However, the contaminant concentration flux ($S_{\varphi 2}$) is solved iteratively at the interface, which makes Method 2 more computationally demanding than Method 1. Method 2 also requires the implementation of the boundary condition at the interface of the coupled model in CFD.

The coupled CFD and analytical methods can also be applied if contaminant source is located close to the first row or the last row of the cabin. Suppose for the case presented in Fig. 1, the contaminant source is located in Row 1 or 2 then, the first 3-rows would be modeled using CFD while the contaminant transmission in the rest of the cabin can be calculated analytically. In such a case Analytical (Domain 1) would not be present and Interface 1 would be a wall (refer to Fig. 1). Interface 2 would be modeled as an inlet with flow similar to the flow in the periodic faces of the single row cabin assuming that we see the end wall effects in the first and/or last 3-rows of a cabin and periodic flow behavior in the rest of the cabin. If the end wall effects are seen for a longer cabin length then more rows have to be simulated using CFD to calculate contaminant transmission with reasonable accuracy.

4. Model Comparison

The applicability of the coupled model and the performance of the two coupling methods were studied using a 30-row, all-economy-class airliner cabin. Figure 4 shows a single row configuration of the twin-aisle cabin model used for the analysis. Two linear inlets at the center supplied conditioned air to both sides of the cabin while the air was extracted through two outlets located at floor level near the side walls. The cabin model, boundary conditions and simulation parameters were similar to those used by Mazumdar and Chen [15]. The following inputs were used for the analytical model [15]:

L_R = Pitch of each row, m = 0.86 m
A_c = Cross section area of the cabin, m^2 = 8.565 m^2
C_{inlet} = Contaminant concentration from the inlet, kg/kg_{air} = 0 kg/kg_{air}
R = Flow rate in L/s per passenger = 10 L/s per passenger
N_R = Number of passengers in each row = 7 passengers

The modified diffusion coefficient of the contaminant (D) computed using the single row cabin model with the procedure outlined in Mazumdar and Chen [15] was 0.006 m^2/s. The longitudinal velocity (V_L) of air flow was 0. The results are analyzed for a contaminant released from the mouth of the center passenger (refer to Fig. 4) seated in the 15th row at a continuous rate of 1.0 X 10^{-6} kg/s.

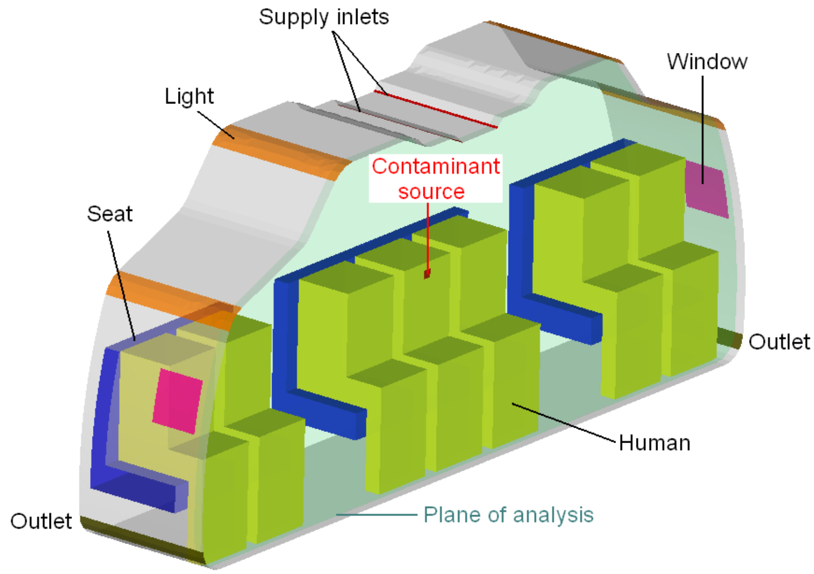

Fig. 4. Schematic of the twin aisle cabin model used for analyses

Figure 5 shows the steady state CFD results of average and maximum contaminant concentrations across the cabin cross-section (the *Plane of analysis* in Fig. 4) along the length of the cabin. The difference between average and maximum contaminant concentrations is the greatest near the contaminant source in row 15, which shows the validity of this method. The difference reduces as we move further from the source location, implying uniform mixing of the contaminant. An asymmetrical contaminant transport in the longitudinal direction is observed as the thermal plume generated by the releasing passenger transfers more contaminant toward the back of the cabin. In order to more quickly capture such local air flow effects on contaminant transmission along the cabin length, the coupled CFD and analytical modeling methods should be used.

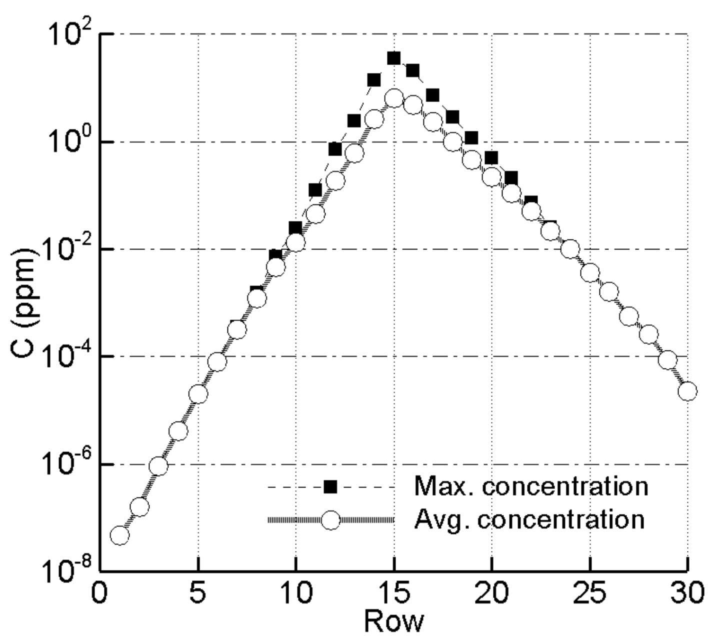

Fig. 5. The maximum and average concentrations across cabin cross-section

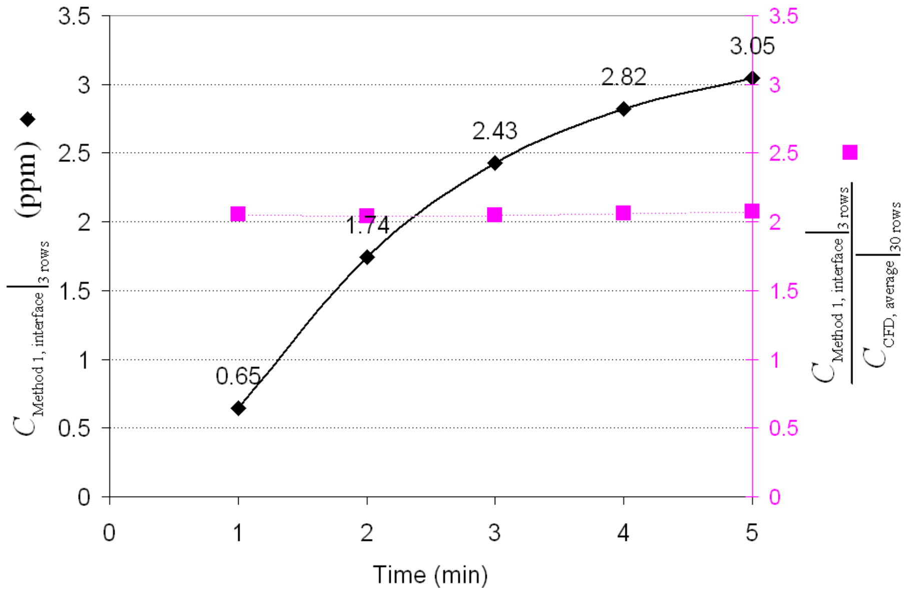

Fig. 6. Comparison of contaminant concentrations at the interface using Method 1 with CFD

Figure 6 compares the simple and time-efficient coupling Method 1 with CFD. The coupled model simulated 3 rows using CFD. The concentration computed, $C_{\text{Method 1, interface}}$, at one of the interfaces of the CFD, and the analytical model is shown at different time instances for a continuously releasing source. The concentration computed at the interface is about two times the actual concentration, $C_{\text{CFD, average}}$, obtained using 30 rows of CFD simulations. The relative error ($C_{\text{Method 1, interface}}$ / $C_{\text{CFD, average}}$) is almost independent of the computing time.

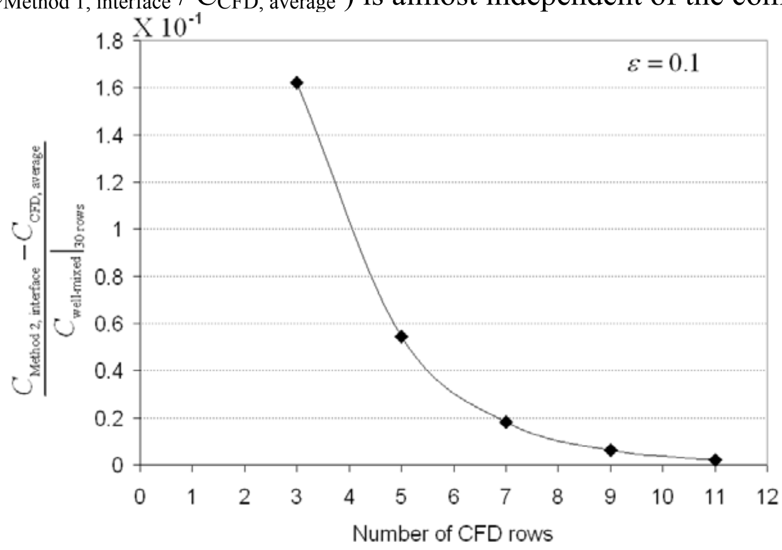

Fig. 7. Comparison of contaminant concentrations at the interface using Method 2 with CFD

Figure 7 shows the difference at steady-state between the actual concentration, $C_{\text{CFD,average}}$, and the concentration predicted at the interface of the CFD and the analytical model, $C_{\text{Method 2, interface}}$, using Method 2. A non-dimensional concentration difference, i.e., the difference in the computed concentration at the interface by the two methods with respect to the concentration in the 30 row cabin under well-mixed conditions ($C_{well\text{-}mixed}$), is shown. The horizontal axis (Number of CFD rows) in the figure signifies the number of rows simulated using CFD for the coupled 30 row CFD-analytical cabin model. For a user-defined convergence criterion of ε = 0.1 (refer to Fig. 3), the error at the interface is an order of magnitude lower than that of the well-mixed concentration. The concentration predicted by Method 2 is much more accurate as contaminant flux at the interface is iteratively balanced. The error at the interface seems to reduce exponentially as more rows are computed using CFD in the coupled model.

A comparison of the accuracy of the coupling methods is presented in Fig. 8. The steady-state non-dimensional concentration difference at the interface is shown. The trend is expected to remain similar for transient contaminant concentration, as is evident in Fig. 6. The difference between the two methods reduced as more rows were computed using CFD. Hence, if more CFD rows are used in the coupled model, Method 1 should be preferred over Method 2, as the second method is more computationally intensive. The computational effort reduction using Method 1 is proportional to the ratio of the number of rows using CFD for the coupled model as well as for the number of rows in a full length cabin. By using the Gaussian elimination scheme to solve the concentration matrix in CFD, the computational effort is reduced by the order of O(1/1000) if 3 rows are computed using CFD for the coupled model in a 30-row cabin [23]. The reduction would be O(27/1000) if the coupled model used 9 CFD rows.

The reduction in computational effort using Method 2 is not easy to quantify, as it is sensitive to a number of parameters: (1) the initial guess about the flux at the interface; (2) the user-defined convergence criterion for the concentration at the interface (ε, refer to Fig. 3); and (3) the mathematical scheme used to update the contaminant flux at the interface between iterations. Such an exhaustive analysis is left as a scope for future investigations. By using the setup mentioned for Method 2 in the Method Implementation section and if 3 rows are computed using CFD for the coupled model in a 30-row cabin, for a transient simulation of 1 minute, the computational time required for Method 2 is about 5 times and 8 times more than the time required for Method 1 for ε of 0.1 and 0.01, respectively. Note: if only steady state contaminant concentrations are to be obtained with the coupled model using Method 2 for a continuous release for an initial guess of $S_{\varphi 2}$ =0 at t = 0 s, the comparative computational times required almost double.

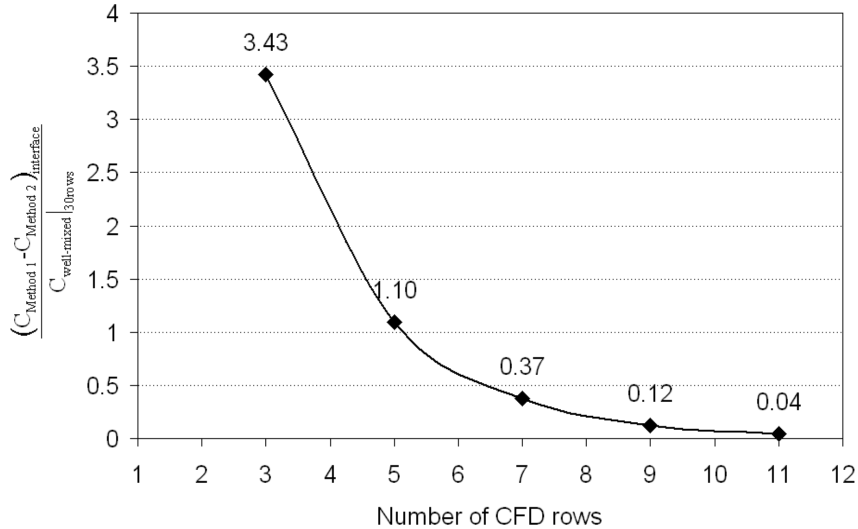

Fig. 8. The difference in steady-state contaminant concentrations predicted at the interface by the two coupling methods

5. Conclusion

This paper has presented a novel coupled CFD and analytical model to compute transient airborne contaminant transmission in a full-length airliner cabin. The coupled model can considerably reduce the amount of computational effort required. The coupled model used CFD near the contaminant source where the concentration was not very uniform across the cross-section; an analytical model is suggested for the rest of the cabin.

This investigation has proposed two different coupling methods: one method assumes outflow condition at the interface of the CFD and the analytical model, while the other iteratively solves the contaminant flux at the interface. The first method is easier to implement and is computationally efficient, but is less accurate. In contrast, the second method is more computationally intensive, but is more accurate. The two methods give similar accuracy as more rows are computed using CFD.

Acknowledgements

This study was partially supported by the National Basic Research Program of China (The 973 Program) through Grant No. 2012CB720100 and the Center for Cabin Air Reformative Environment (CARE) at Tianjin University, China. This investigation was also partially funded by the U.S. Federal Aviation Administration (FAA) Office of Aerospace Medicine through the National Air Transportation Center of Excellence for Research in the Intermodal Transport Environment at Purdue University under Cooperative Agreement 10-C-RITE-PU. Although FAA sponsored this project, it neither endorses nor rejects the findings of the research. This information is presented in the interest of invoking comments from the technical community about the results and conclusions of the research.

References

1 Joseph SMP, Kwok YY, Albert DMEO, Klaus S: The Severe Acute Respiratory Syndrome: New England Journal of Medicine 2003; 349(25):2431-41.
2 Mangili A, Gendreau MA: Transmission of infectious disease during commercial air travel: Lancet 2005; 365:989-96.
3 Musher DM: How contagious are common respiratory tract infections? New England Journal of Medicine 2003; 348:1256-66.
4 Centers for Disease Control and Prevention: Update: Multistate Outbreak of Mumps - United States, January 1-May 2, 2006, http://www.cdc.gov/mmwr/.
5 Mazumdar S, Poussou S, Lin C-H, Isukapalli SS, Plesniak MW, Chen Q: The impact of scaling and body movement on contaminant transport in airliner cabins: Atmospheric Environment 2011; 45(33):6019-6028.
6 Zhang Z, Chen X, Mazumdar S, Zhang T, Chen Q: Experimental and numerical investigation of airflow and contaminant transport in an airliner cabin mockup: Building and Environment 2009; 44(1):85-94.
7 Liu W, Wen J, Chao J, Yin W, Shen C, Lai D, Lin C-H, Liu J, Sun H, Chen Q: Accurate and high-resolution boundary conditions and flow fields in the first-class cabin of an MD-82 commercial airliner: Atmospheric Environment 2012; 56, 33-44.
8 Mazumdar S, Chen Q: Influence of cabin conditions on placement and response of contaminant detection sensors in a commercial aircraft: Journal of Environmental Monitoring 2008; 10:71-81.
9 Zhai, Z: Application of computational fluid dynamics in building design: aspects and trends: Indoor and Built Environment 2006; 15(4):305-313.
10 Zhai Z, Metzger ID: Taguchi-method-based CFD study and optimisation of personalised ventilation Systems: Indoor and Built Environment 2012; 21:690-702.
11 Megri AC, Haghighat F: Zonal modeling for simulating indoor environment of buildings: review, recent developments, and applications: HVAC&R Research 2007; 13, 887–905.
12 Wang H, Zhai Z: Application of coarse-grid computational fluid dynamics on indoor environment modeling: Optimizing the trade-off between grid resolution and simulation accuracy: HVAC&R Research 2012; 18, 915-933.
13 Zuo W, Chen, Q: Fast and informative flow simulations in a building by using fast fluid dynamics model on graphics processing unit: Building and Environment 2010; 45(3), 747-757.
14 Thomas B, Soleimani-Mohseni M: Artificial neural network models for indoor temperature prediction: investigations in two buildings: Neural Computing and Applications 2007; 16, 81–89.
15 Mazumdar S, Chen Q: A one-dimensional analytical model for airborne contaminant transport in airliner cabins: Indoor Air 2009; 19(1), 3-13.
16 National Research Council: The Airliner Cabin Environment and the Health of Passengers and Crew: National Academy Press, Washington, DC.
17 Yan W, Zhang Y, Sun Y, Li D: Experimental and CFD study of unsteady airborne pollutant transport within an aircraft cabin mock-up: Building and Environment 2009; 44(1):34-43.
18 Carslaw HS, Jaeger JC: Conduction of heat in solids: Oxford University Press, Amen House, London, 1959.

19 Ozisik MN: Boundary Value Problems of Heat Conduction. International Textbook Company, Pennsylvania, 1968.
20 Powers DL: Boundary Value Problems and Partial Differential Equation. Elsevier Academic Press, 2006.
21 ANSYS: ANSYS Fluent 12.0 Documentation: ANSYS Fluent Inc., Lebanon, NH, 2009.
22 Mathews JH: Numerical methods for mathematics, science and engineering. Prentice Hall College Div. 1994.
23 Cohn H, Kleinberg R, Szegedy B, Umans C: Group-theoretic algorithms for matrix multiplication. Proceedings of the 46th Annual Symposium on Foundations of Computer Science, Pittsburgh, PA, IEEE Computer Society, 2005, 379–388.